Journal of Alloys and Compounds 506 (2010) 593–599

Contents lists available at ScienceDirect

Journal of Alloys and Compounds

journal homepage: www.elsevier.com/locate/jallcom

The microstructure parameters and microhardness of directionally solidified Ti–43Al–3Si alloy

Jianglei Fan*, Xinzhong Li, Yanqing Su, Jingjie Guo, Hengzhi Fu

School of Material Science and Engineering, Harbin Institute of technology, Harbin, Heilongjian 150001, PR China

ARTICLE INFO

Article history:
Received 30 May 2010
Received in revised form 15 July 2010
Accepted 15 July 2010
Available online 22 July 2010

Keywords:
TiAl-based alloy
Directional solidification
Seeding materials
Intermetallics
Microhardness

ABSTRACT

TiAl-based alloy (Ti–43Al–3Si at.%) was directionally solidified at a constant temperature gradient (G = 20 K/mm) in a wide range of growth rates (5–60 μm/s) by using a Bridgman type directional solidification furnace. The cellular spacing (λ), lamellar spacing (λ_L), volume fraction of Ti_5Si_3 phases (f_V) and microhardness (H_V) were measured. The values of λ, λ_L and f_V decrease with increasing growth rate (V). The value of H_V increases with the increasing values of V and $\lambda_L^{-0.5}$, and decreases with the increasing values of λ, and f_V. The dependence of H_V on V, λ, $\lambda_L^{-0.5}$ and f_V was determined by linear regression analysis. The fitted exponent values obtained in this work were compared with the previous experimental results for similar alloy systems.

1. Introduction

Intermetallic γ-TiAl-based alloys are considered to be a new generation of high temperature structural materials for aerospace and automotive industries due to their low density, good oxidation resistance and high temperature strength [1–4]. Of the numerous microstructures that can be formed in TiAl-based alloys, the fully lamellar microstructures consisting of TiAl (γ-phase) and Ti_3Al (α_2-phase) have displayed a good combination of room temperature toughness, ductility, creep strength and elevated temperature strength [5,6].

As was shown in the literature [5,7–10], TiAl-based alloys with aligned lamellar orientation have a good combination of strength and ductility in a wide range of temperature. The main challenge is that the lamellar microstructure is not form from the liquid but from the solid-state transformation [5,7–10]. During cooling the γ phases form from the matrix α phases according to the crystallographic orientation relationship of $(1\,1\,1)_\gamma//(0\,0\,0\,1)_\alpha$. Due to the preferred growth direction of α phase is [0 0 0 1], the lamellar orientation is perpendicular to the growth direction. Hence, to obtain the preferred lamellar orientation, the orientation of high temperature α phase must first be controlled [8–11]. However, the aligned lamellar orientation can be obtained by directional solidification and seeding techniques with a seed having specific α orientation [7,9,11–14,5]. One of the main factors for this technique is to found a suit seeding materials. As a seed material, the primary solidification phase must be α phase and the original lamellar orientation should be restored during heating to and cooling from single-phase α-region [8,14]. According to the literature [5,7,9,12,15], Ti–43Al–3Si(at.%) alloy is identified to be a suitable seed material which is used to control the orientation of lamellar structures in TiAl alloys. However, the evolution of microstructure characteristics for Ti–43Al–3Si(at.%) alloy during directional solidification has not been well understood. The microstructure characteristics of Ti–43Al–3Si(at.%) alloy are important to the controlling of lamellar orientation of TiAl-based alloys during directional solidification. Unfortunately, little work has been reported about the microstructure characteristics of directionally solidified Ti–43Al–3Si(at.%) alloy.

As reported by Lapin et al. [6,15], there is a linear relationship between microhardness and yield stress, which promises the mechanical properties of directionally solidified TiAl ingots to be predicted from the values of Vickers microhardness. Similar linear dependence of the yield stress on the hardness was also observed in wrought TiAl alloy with fully lamellar structures [16]. It appears that the microhardness analysis offers a relatively simple method to predict the mechanical properties of materials [17]. The values of Vickers microhardness are useful for quality control in the production of directionally solidified TiAl alloys.

The purpose of this work is to study the evolution of microstructure characteristics and microhardness for Ti–43Al–3Si(at.%) alloy during directional solidification. In this paper, directionally solidified Ti–43Al–3Si(at.%) alloy has been carried out to experimentally investigate the effect of growth rate (V) on the cellular spacing

* Corresponding author. Tel.: +86 0451 86418815; fax: +86 0451 86415776.
E-mail address: JLFan2011@163.com (J. Fan).

0925-8388/$ – see front matter © 2010 Elsevier B.V. All rights reserved.
doi:10.1016/j.jallcom.2010.07.122

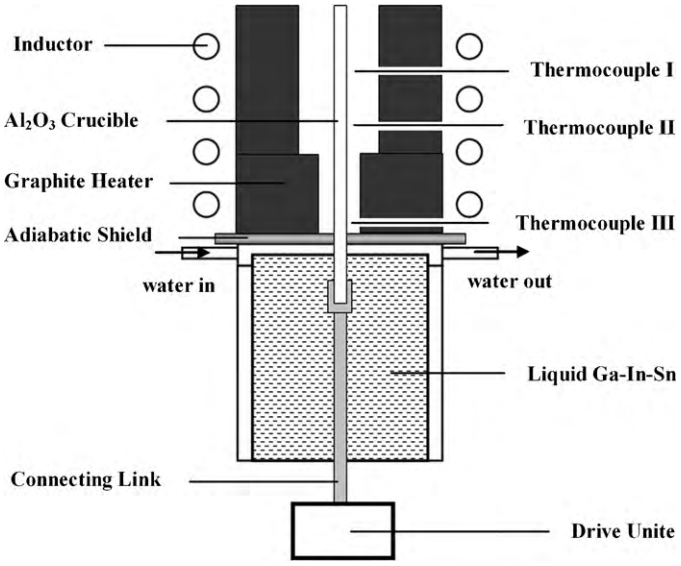

Fig. 1. Schematic of Bridgman type directional solidification furnace.

(λ), interlamellar spacing (λ_L) and volume fraction of Ti_5Si_3 phases (f_V) during the directional solidification. The dependences of the microhardness (H_V) on the growth rate (V), cellular spacing (λ), interlamellar spacing (λ_L) and volume fraction of Ti_5Si_3 phases (f_V) are also studied.

2. Experimental procedures

Master ingot with nominal composition of Ti–43Al–3Si(at%) alloy was prepared by using Ti (99.96%), Al (99.99%) and Si (99.96%) of commercial purity in a cold crucible induction furnace under argon atmosphere. The samples were machined to rods with 3 mm diameter and 100 mm in length from the ingot by a spark machining. The directional solidification (DS) experiments were performed in Bridgman-type system. The schematic diagram of Bridgman type directional solidification furnace is shown in Fig. 1. The apparatus consisted of an induction coil, a graphite heater, a water cooled liquid metal bath filled with a liquid Ga–In–Sn alloy and an adiabatic zone which is located between the heater and the cooler. The temperature gradient was measured by W/Re thermocouples that were placed near the outside surface of the alumina tubes, as shown in Fig. 1. The temperature gradient close to the solid/liquid interface was measured to be approximately 20 K/mm. The samples are placed into 99.99 pct pure alumina crucibles of 4/5.5 mm diameter (insider/outside diameter) and length of 150 mm. Each specimen was heated to 1723 K during 4 h and held for different time before directional solidification, and then was directionally solidified with growth rate range from 5 μm/s to 60 μm/s. The growth length of the samples is 40 mm during directional solidification. At the end of the experiment, the sample was quenched into the liquid Ga–In–Sn alloy to restored the solid/liquid interface.

After directional solidification, the longitudinal and transverse section of the specimens were cut, polished and etched with a solution of 10 ml HF-10 ml HON_3-180 ml H_2O for further analysis. After metallographic process, the microstructures of the samples were revealed and photographed with optical microscope. Fig. 2 shows the typical images of optical microscope.

The cellular spacings were measured from the photographs according to the method described in Refs. [18,19]. The interlamellar spacings were measured from the SEM back scattered electron (BSE) images according to the method described in Ref. [20]. The value of interlamellar spacing is the thickness of one α lamellae and γ lamellae nearby. Fig. 2 shows the typical BSE images of lamellar structures. The measured values are the average values and given in Table 1.

Microhardness measurements were made with a standardized Vickers measuring test device using 100 g load and a dwell time of 10 s on the longitudinal section. The microhardness is average of at least 15 measurements. The values of H_V are also given in Table 1.

3. Results and discussion

3.1. Microstructure of directionally solidified ingots

The microstructure of the directionally solidified specimen consisted of $\alpha_2(Ti_3Al)/\gamma(TiAl)$ lamellar structures and ξ-Ti_5Si_3 phases, as shown in Fig. 2. The chemical composition analysis of the phases in the samples was carried out by using energy dispersive X-ray analysis (EDX) and is given in Fig. 3. According to EDX results and the solubility of components in phase, the black phases are γ phase, the gray ones are α_2 phase and the white are Ti_5Si_3 phase. Fig. 4 shows the calculated partial isopleth diagram of Ti–Al–Si ternary system at 3.5 at.% Si after Manesh and Flower [21]. The lamellar structures formed by eutectoid reaction: $\alpha \rightarrow \alpha_2 + \gamma$. Due to the low solubility of Si in the matrix, some isolated large Ti_5Si_3 rods formed in the Si-rich region of the liquid phase by reaction of $L \rightarrow \xi$. The eutectic Ti_5Si_3 phase formed by reaction: $L \rightarrow \alpha + \xi$ and $L \rightarrow \gamma + \xi$, as described in Ref. [22]. In addition, some Al_2O_3 particles that formed by the reaction between the crucible and the alloy were observed in the directionally solidified specimens, which were shown in Fig. 2(a2, c2 and d2). The solid–liquid interface and microstructure evolution of Ti–43Al–3Si(at.%) alloy was studied in previous works [22,23].

3.2. Effect of growth rate on the cellular spacing, the interlamellar spacing and volume fraction of Ti_5Si_3 phases

Fig. 5 shows the variations of the cellular spacing (λ), interlamellar spacing (λ_L) and volume fraction of Ti_5Si_3 phases (f_V) with the growth rate (V) at a constant temperature gradient (G = 20 K/mm). The error bars indicate the errors in the λ values, λ_L values and f_V values, which are in the range of ±2%, ±2.5% and ±2%. The values of λ, λ_L and f_V decrease with the increasing the values of V at constant G. The value of f_V decreases from 12.2 to 8.9 pct with increasing growth rate (V) from 5 μm/s to 60 μm/s at constant G. The largest f_V (12.5%) was obtained at the growth rate (V = 10 μm/s), which is greater than the value of 9.3% obtained by Sun et al. [24] for Ti–48Al–3Si(at.%) alloy. The relationship between λ, $\lambda_L{}^{-0.5}$, f_V and V was obtained by using linear regression analysis, the results were given as:

$$\lambda = 650.1\, V^{-0.44} \quad (1)$$

$$\lambda_L = 13.2\, V^{-0.41} \quad (2)$$

$$f_V = 16.6\, V^{-0.17} \quad (3)$$

The regression coefficient of this fit is r^2 = 0.97, 0.99 and 0.87, respectively.

The exponent value of growth rate (V) for λ was fitted to be 0.44 that is small than the theoretical value of 0.5, 0.5 and 0.59 resulting from the model of Okamoto–Kishitake [25], Bouchard–Kirkaldy [26] and Hunt–Lu [27], respectively. However, the exponent value is greater the theoretical value of 0.25 from the models of Hunt [28], Kruz–Fisher [29], Kruz–Fisher [30] and Trivedi Model [31], respectively. The exponent value of interlamellar spacing is greater than 0.24 obtain by Lapin et al. [6] for Ti–46Al–2W–0.5Si(at.%) alloy.

The volume fraction of Ti_5Si_3 phase decrease with increasing growth. It is because that the rejection of solute was restrained with increasing growth rate, which cause the decreasing of the concentration of Si in the liquid phase. Therefore, the formation of Ti_5Si_3 phase was reduced and the volume fraction of Ti_5Si_3 phase decreased.

3.3. Dependency of the microhardness on the growth rate, cellular spacing, lamellar spacing and volume fraction of Ti_5Si_3 phase

Fig. 6 shows the variations of the microhardness (H_V) with the growth rate (V), cellular spacing (λ), lamellar spacing (λ_L) and volume fraction of Ti_5Si_3 (f_V) phases at a constant temperature gradient (G = 20 K/mm). The error bars indicate the errors in the values of H_V, λ and f_V, which are in the range of ±1%, ±2% and ±2%, respectively. The value of H_V increases with the increasing the values of V at constant G, as shown in Fig. 6a. The value of H_V increases with the

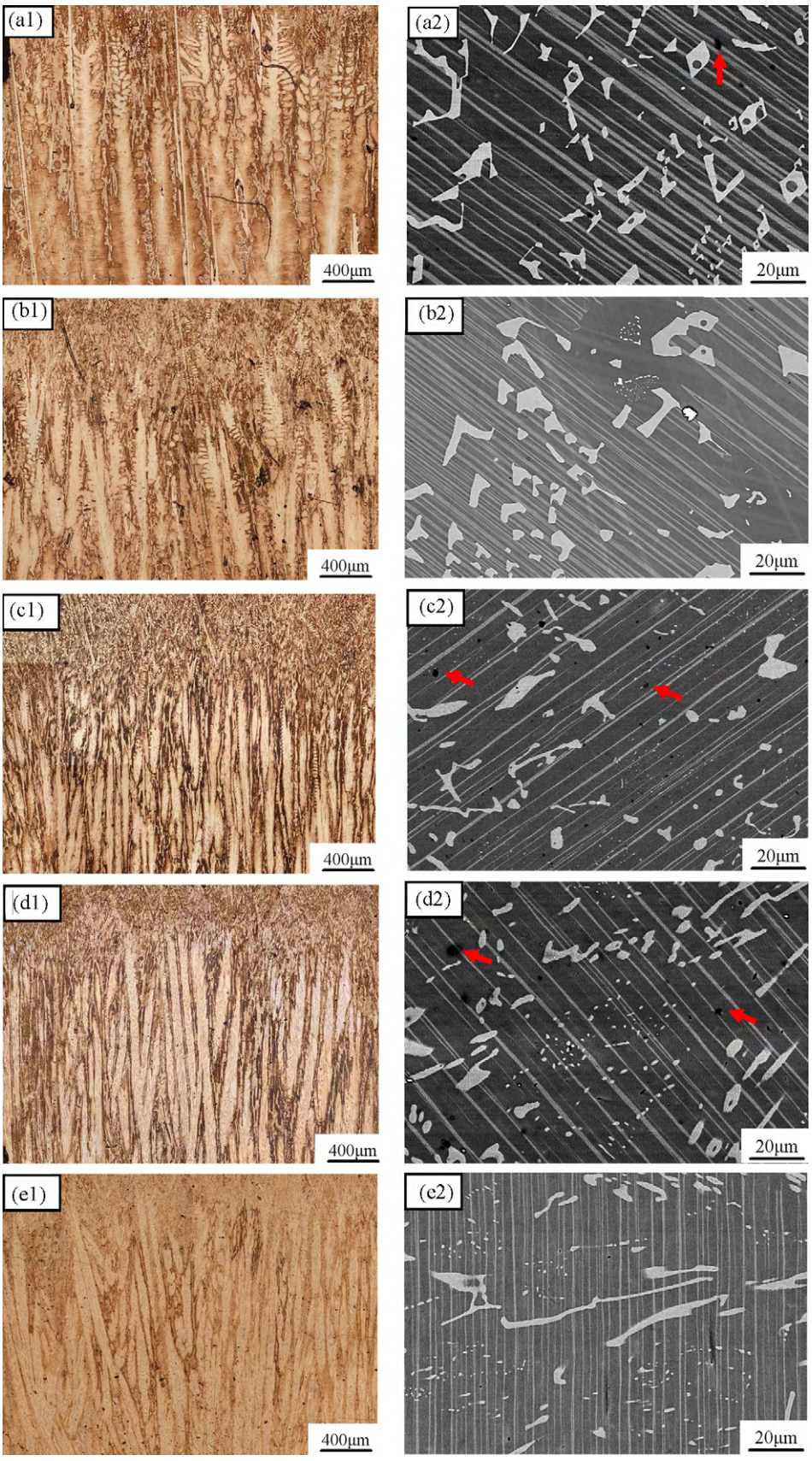

Fig. 2. Images of growth morphologies of directionally solidified Ti–43Al–3Si(at.%) alloy with different growth rates in constant temperature gradient (G = 20 K/mm): (a) V = 5 μm/s; (b) V = 10 μm/s; (c) V = 20 μm/s; (d) V = 30 μm/s; (e) V = 60 μm/s. The left sides are corresponded to optical images of longitudinal section at solid–liquid interface; right sides corresponded to BSE images of transverse section, respectively. The arrows indicate the Al_2O_3 particles.

Table 1
The values of cellular spacing, lamellar spacing and microhardness for directionally solidified Ti–43Al–3Si(at.%) alloy at various growth rate with constant temperature gradient (G = 20 K/mm).

Solidification parameters		Cellular spacing	Lamellar spacing	Volume fraction of Ti_5Si_3 phases	Microhardness
G (K/mm)	V (μm/s)	λ (μm)	λ_L (μm)	f_V (%)	H_V
20	5	371.7	6.88	12.2	420.4
	8	210.7	5.41	11.8	434.6
	10	238.2	5.31	12.5	460.7
	15	192.0	4.68	11.4	479.8
	20	187.3	3.76	9.1	496.3
	25	169.0	3.44	10.2	480.8
	30	133.8	3.34	8.1	503.2
	40	135.8	2.67	9.1	524.2
	50	100.4	2.71	8.8	512.1
	60	120.0	2.54	8.9	549.4

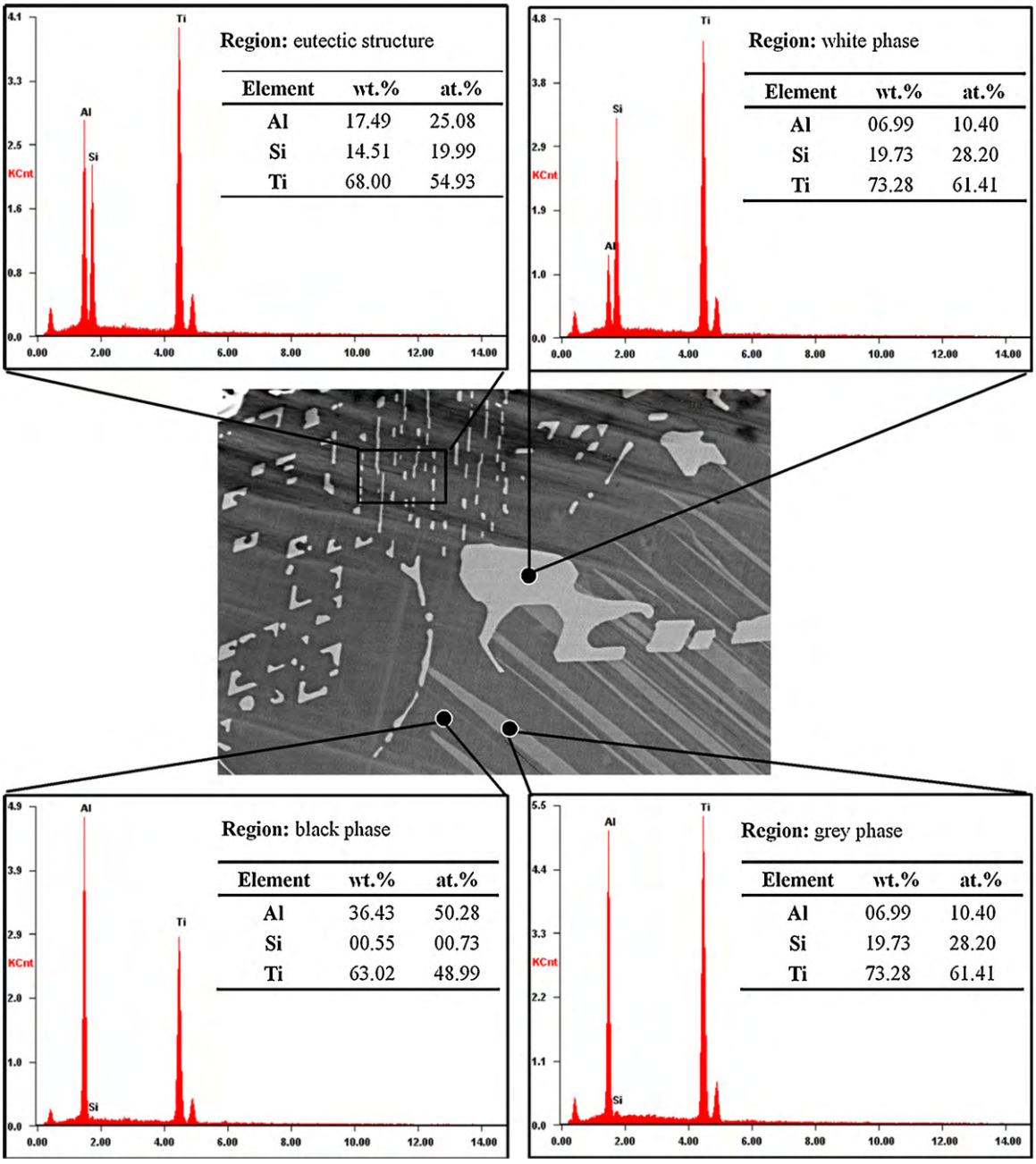

Fig. 3. The chemical composition analysis of Ti–43Al–3Si(at.%) alloy by using SEM EDX, the black phases are γ-TiAl phase, the grey phases are α_2-Ti_3Al phase, the white phases are ξ-Ti_5Si_3 phase.

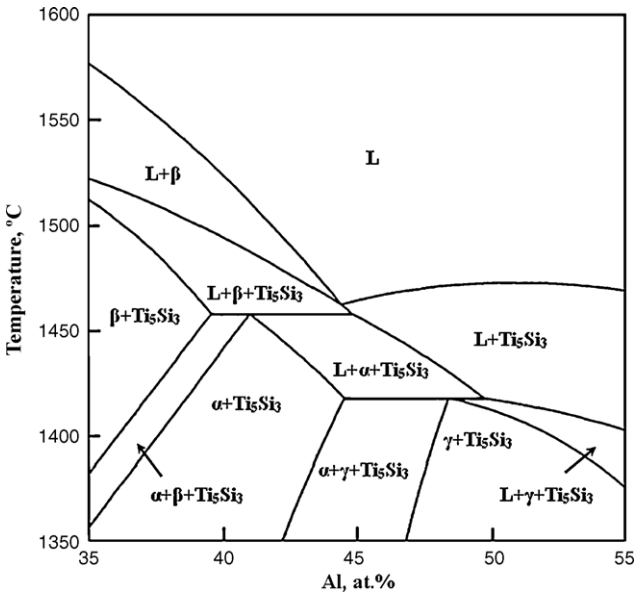

Fig. 4. The calculated partial isopleth diagram of Ti–Al–Si ternary system at 3.5 at.% Si after Manesh and Flower [22].

increasing the value of $\lambda_L^{-0.5}$, according to a Hall–Petch type relationship in the form of $H_V = H_{V0} + k\lambda_L^{-0.5}$ [6,16,32], where H_{V0} and k are materials constants. It was found that the value of H_V decreases with increasing λ and f_V. The dependence of the H_V on V, λ, $\lambda_L^{-0.5}$ and f_V was determined by using linear regression analysis, and the results were given as:

$$H_V = 363.1\,V^{0.10} \quad (4)$$

$$H_V = 1288.2\lambda^{-0.19} \quad (5)$$

$$H_V = 257.5 + 0.44\lambda_L^{-0.5} \quad (6)$$

$$H_V = 1318.3 f_V^{-0.44} \quad (7)$$

The regression coefficients are $r^2 = 0.96$, 0.90, 0.95, and 0.83, respectively.

The exponent value of growth rate (V) is 0.10 that is in smaller than the value of 0.14 and 0.15 obtained by Lapin et al. [6] for Ti–46Al–2W–0.5Si(at.%) alloy and Fan et al. [33] for Ti–46Al–0.5W–0.5Si(at.%) alloy, respectively. The exponent value of cellular spacing (λ) is 0.19 that is smaller than the value of 0.31 obtained by Fan et al. [33] for Ti–46Al–0.5W–0.5Si(at.%) alloy.

With increasing of the growth rate, the cellular spacing (λ) decreased and the columnar grains were refined. The strength of the directionally solidified Ti–43Al–3Si(at.%) was enhanced by fine grains. Consequently, the microhardness (H_V) increased with decreased cellular spacing (λ). During the directional solidification, element of Si rejected in the liquid phase between the dendrites due to the low solubility of Si in the α_2/γ lamellar structures. The Ti_5Si_3 phase formed in the Si-rich region of the liquid by the reaction of by $L \rightarrow Ti_5Si_3$. With increasing growth rate, the cooling rate increased and the rejection of Si was restrained. Hence, the volume fraction (f_V) of Ti_5Si_3 phase decreased. The concentration of Si in the α_2/γ lamellar structures increased, which has solution strengthen effect for the Ti–43Al–3Si(at.%) alloy. Therefore, the microhardness (H_V) increased with decreased of f_V.

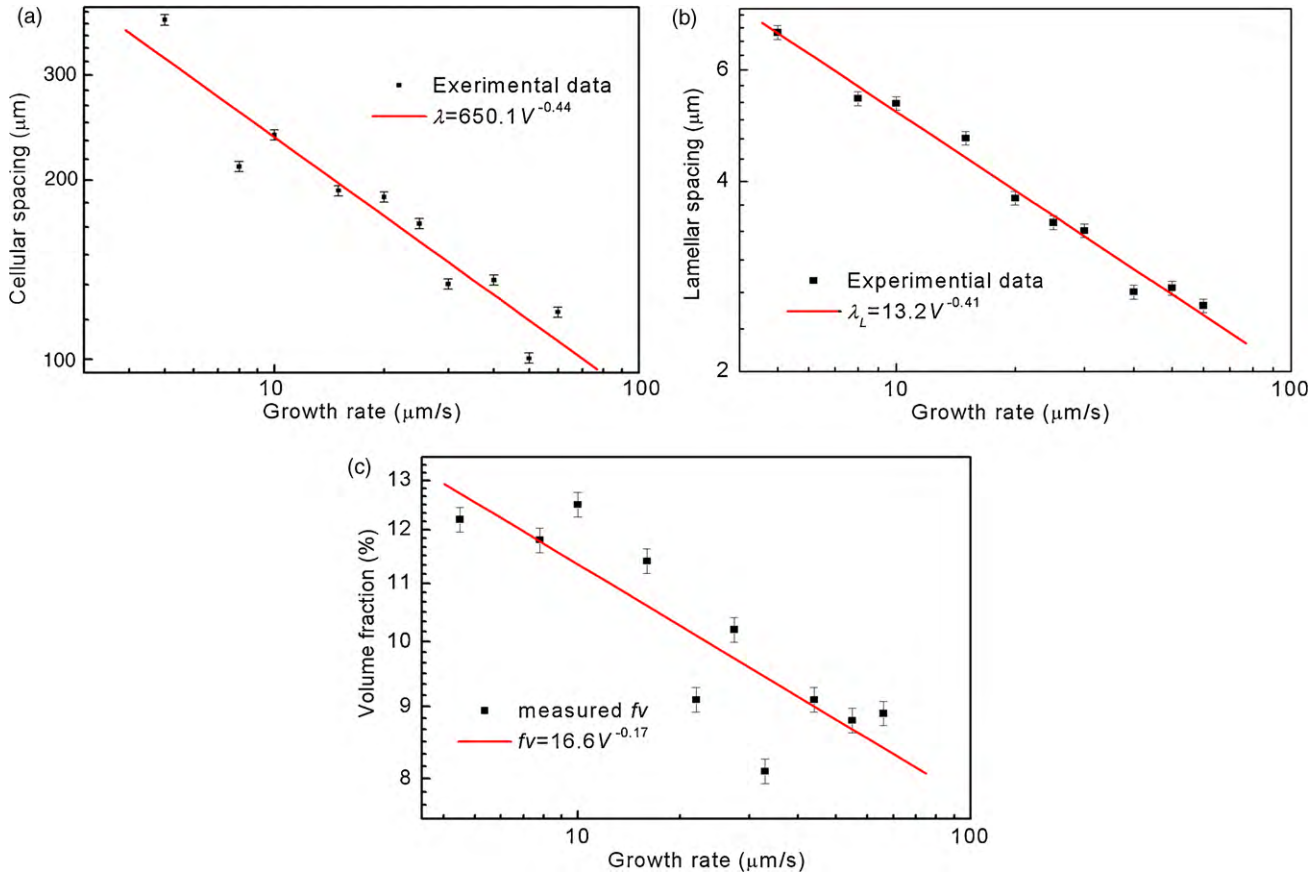

Fig. 5. Effects of growth rate on the cellular spacing (a), the lamellar spacing (b) and the volume fraction of Ti_5Si_3 phases (c) of directionally solidification Ti–43Al–3Si(at.%) alloy at a constant temperature gradient (G = 20 K/mm).

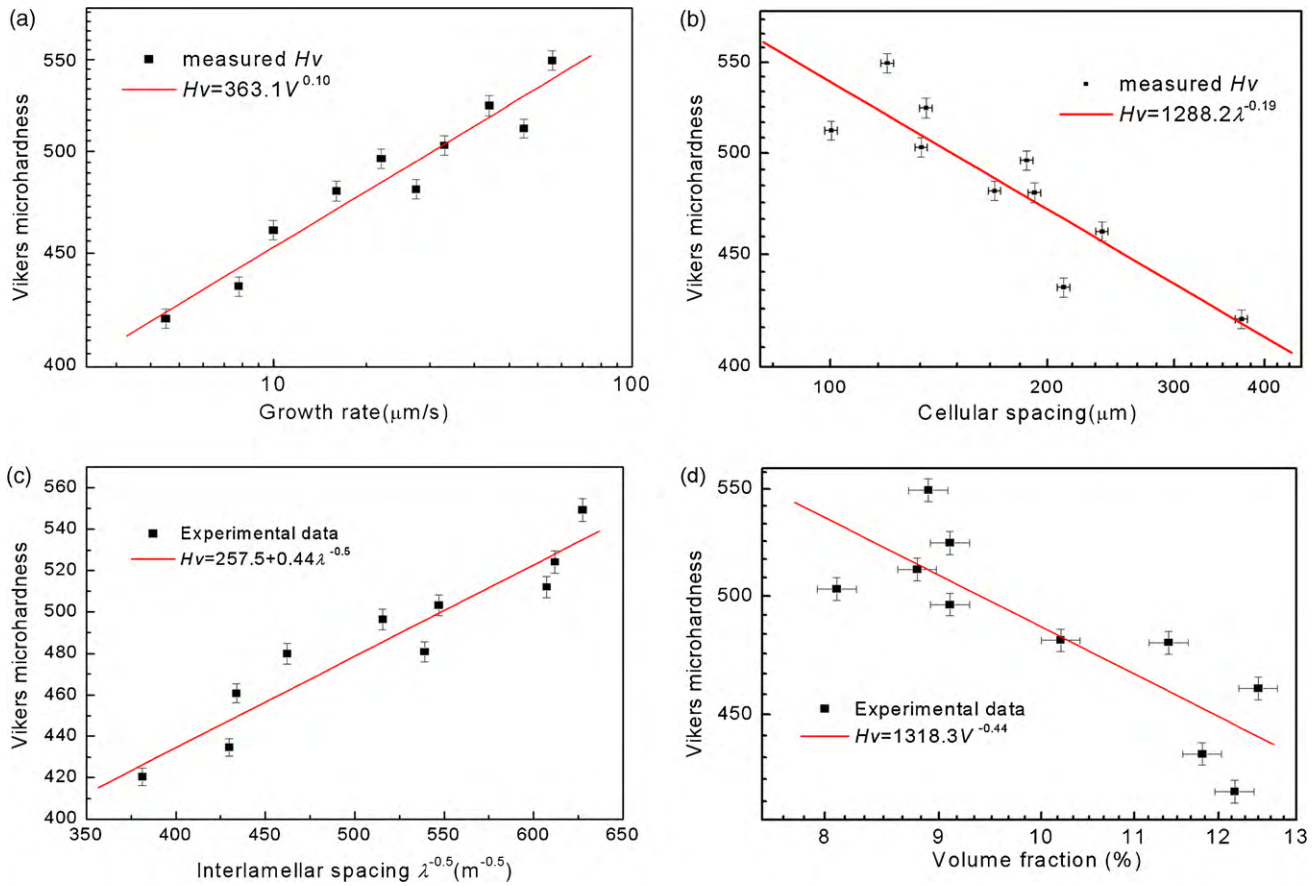

Fig. 6. The variation of microhardness as a function of growth rate (a), cellular spacing (b), reciprocal square root of interlamellar spacing (c), and volume fraction of Ti_5Si_3 phases (d) for directionally solidification Ti–43Al–3Si(at.%) alloy at a constant temperature gradient (G = 20 K/mm).

4. Conclusions

In the present work, the microstructure parameters and microhardness of directionally solidified Ti–43Al–3Si(at.%) alloy were investigated. The following conclusions were reached:

(1) The values of cellular spacing (λ), interlamellar spacing (λ_L) and volume fraction of (f_V) alloy decrease with increasing growth rate (V) for directionally solidified Ti–43Al–3Si(at.%). The relationships were given as follows:

$$\lambda = 650.1\,V^{-0.44}$$
$$\lambda L = 13.2\,V^{-0.41}$$
$$f_V = 16.6\,V^{-0.17}.$$

(2) The valuable of microhardness (H_V) increases with increasing growth rate (V) and the reciprocal square root of interlamellar spacing ($\lambda_L{}^{-0.5}$) for directionally solidified Ti–43Al–3Si(at.%) alloy. The relationships can be given as:

$$H_V = 363.1\,V^{0.10}$$
$$H_V = 257.5 + 0.44\lambda L^{-0.5}.$$

(3) The valuable of microhardness (H_V) decreases with increasing cellular spacing (λ) and volume fraction of Ti_5Si_3 phase (f_V) for directionally solidified Ti–43Al–3Si(at.%) alloy. The relationships were given as:

$$H_V = 1288.2\lambda^{-0.19}$$
$$H_V = 1318.3 f_V{}^{-0.44}.$$

Acknowledgements

This project was supported by National Science Foundation of China (Nos. 50771041 and 50801019) and Post-doctor Foundation of China (No. 20080430909).

References

[1] X. Wu, Review of alloy and process development of TiAl alloys, Intermetallics 14 (2006) 1114–1122.
[2] H. Clemens, H. Kestler, Processing and Applications of intermetallic γ-TiAl-based alloys, Adv. Eng. Mater. 2 (2000) 551–570.
[3] D.M. Dimiduk, Gamma titanium aluminide alloys – an assessment within the competition of aerospace structural materials, Mater. Sci. Eng. A263 (1999) 281–288.
[4] Y.W. Kim, Ordered intermetallic alloys, part III: gamma titanium aluminide, J. Met. (1994) 30–39.
[5] D.R. Johnson, H. Inui, M. Yamaguchi, Directional solidification and microstructural control of the TiAl/Ti_3Al lamellar microstructure in TiAl–Si alloys, Acta Mater. 44 (1996) 2523–2535.
[6] J. Lapin, L. Ondrúš, M. Nazmy, Directional solidification of intermetallic Ti–46Al–2W–0.5Si alloy in alumina moulds, Intermetallics 10 (2002) 1019–1031.
[7] S.E. Kim, Y.T. Lee, M.H. Oh, H. Inui, M. Yamaguchi, Directional solidification of TiAl–Si alloys using a polycrystalline seed, Intermetallics 8 (2000) 399–405.
[8] D.R. Johnson, H. Inui, S. Muto, Y. Omiya, T. Yamanaka, Microstructural development during directional solidification of α-seed TiAl alloys, Acta Mater. 54 (2006) 1077–1085.
[9] T. Yamanaka, D.R. Johnson, H. Inui, M. Yamaguchi, Directional solidification of TiAl–Re–Si alloys with aligned γ/$α_2$ lamellar microstructures, Intermetallics 7 (1999) 779–784.
[10] H. Fu, J. Guo, Y. Su, D. Xu, J. Li, Directional solidification and lamellar orientation control of TiAl intermetallics, Chin. J. Nonferrous Met. 13 (2003) 797–910.
[11] H.N. Lee, D.R. Johnson, H. Hnui, M.H. Oh, D.M. Wee, M. Yamaguichi, Microstructure control though seeding and directional solidification of TiAl alloys containing Mo and C, Acta Mater. 48 (2000) 3221–3233.

[12] D.R. Johnson, Y. Masuda, H. Inui, M. Yamaguchi, Alignment of the TiAl/Ti_3Al lamellar microstructure in TiAl alloys by directional solidification, Mater. Sci. Eng. A239–240 (1997) 577–583.
[13] M. Yamaguichi, D.R. Johnson, H.N. Lee, H. Inui, Directional solidification of TiAl-based alloys, Intermetallics 8 (2000) 511–517.
[14] H.N. Lee, D.R. Johnson, H. Inui, M.H. Oh, D.M. Wee, M. Yamaguchi, A composition window in the TiAl–Mo–Si system suitable for lamellar structure control through seeding and directional solidification, Mater. Sci. Eng. A329–331 (2002) 19–24.
[15] J. Lapin, L. Ondrúš, O. Bajana, Effect of Al_2O_3 particles on mechanical properties of directionally solidified interlametallic Ti–46Al–2W–0.5Si alloy, Mater. Sci. Eng. A360 (2003) 85–95.
[16] D.M. Dimiduk, P.M. Hazzledine, T.A. Parthasarathy, S. Seshagiri, M.G. Mendiratta, The role of grain size and selected microstruetural parameters in strengthening fully lamellar TiAl alloys, Metall. Mater. Trans. A 29 (1998) 37–47.
[17] P. Christodoulou, M. Garbiak, B. Piekarski, Materials microhardness "finger prints", Mater. Sci. Eng. A457 (2007) 350–367.
[18] H. Kaya, M. Gündüz, E. Çadırlı, N. Maraşlı, Dependency of microindentation hardness on solidification processing parameters and cellular spacing in the directionally solidified Al based alloys, J. Alloys Compd. 478 (2009) 281–286.
[19] U. Böyük, N. Maraşlı, The microstructure parameters and microhardness of directionally solidified Sn–Ag–Cu eutectic alloy, J. Alloys Compd. 485 (2009) 264–269.
[20] E. Çadırlı, H. Kaya, M. Gündüz, Effect of growth rates and temperature gradients on the lamellar spacing and undercooling in the directionally solidified Pb–Cd eutectic alloy, Mater. Res. Bull. 38 (2003) 1457–1476.
[21] S.H. Manesh, H.M. Flower, Liquidus projection of Ti–Al–Si ternary system in vicinity of gamma alloys, Mater. Sci. Technol. 10 (1994) 674–679.
[22] X.Z. Li, J.L. Fan, J.J. Guo, Y.Q. Su, H.Z. Fu, Structure evolution of directionally solidified Ti–43Al–3Si alloy II. Microstructure evolution in the steady-state growth region, Acta Metall. Sin. 45 (2009) 308–313.
[23] J.L. Fan, X.Z. Li, J.J. Guo, Y.Q. Su, H.Z. Fu, Structure evolution of directionally solidified Ti–43Al–3Si alloy I. Microstructure evolution in the transition region, Acta Metall. Sin. 45 (2009) 302–307.
[24] F.S. Sun, C.X. Cao, S.E. Kim, Y.T. Lee, M.G. Yan, Ti_5Si_3 whisker in-situ reinforced TiAl alloys, Metall. Mater. Trans. A 32 (2001) 1233–1243.
[25] T. Okamoto, K. Kishitake, Dendritic structure in unidirectionally solidified aluminum, tin, and zinc base binary alloys, J. Cryst. Growth 29 (1975) 137–146.
[26] D. Bouchard, J.S. Kirkaldy, Prediction of dendrite arm spacings in unsteady-and steady-state heat flow of unidirectionally solidified binary alloys, Metall. Mater. Trans. B28 (1997) 633–651.
[27] J.D. Hunt, S.Z. Lu, Numerical modeling of cellular/dendritic array growth: spacing and structure predictions, Metall. Mater. Trans. A 27A (1996) 611–623.
[28] J.D. Hunt, Solidification and Casting of Metals, The Metals Society, London, 1979, p. 9.
[29] W. Kurz, D.J. Fisher, Dendritic growth at the limit of stability: tip radius and spacing, Acta Metall. Mater. 29 (1981) 11–20.
[30] W. Kruz, D.J. Fisher, Fundamentals of Solidification, Trans Techblications, Aedermannsdorf, Switzerland, 1989, p. 86.
[31] R. Trivedi, Interdendritic spacing. Part II. A comparison of theory and experiment, Metall. Mater. Trans. A15 (1984) 977–982.
[32] J. Lapin, Effect of lamellar structure on microhardness and yield stress of directionally solidified intermetallic Ti–46Al–0.5W–0.5Si alloy, J. Mater. Sci. Lett. 22 (2003) 747–749.
[33] J. Fan, X. Li, Y. Su, J. Guo, H. Fu, Dependency of microhardness on solidification processing parameters and microstructure characteristics in the directionally solidified Ti–46Al–0.5W–0.5Si alloy, J. Alloys Compd. 504 (2010) 60–64.